

1 **Interpreting UniFrac with Absolute Abundance: A Conceptual and Practical Guide**

2 Augustus Pendleton^{1*} & Marian L. Schmidt^{1*}

3 ¹Department of Microbiology, Cornell University, 123 Wing Dr, Ithaca, NY 14850, USA

4 **Corresponding Authors:** Augustus Pendleton: arp277@cornell.edu; Marian L. Schmidt:
5 marschmi@cornell.edu

6 **Author Contribution Statement:** Both authors contributed equally to the manuscript.

7 **Preprint servers:** This article was submitted to *bioRxiv* (doi: 10.1101/2025.07.18.665540) under
8 a CC-BY-NC-ND 4.0 International license.

9 **Keywords:** Microbial Ecology - Beta Diversity - Absolute Abundance - Bioinformatics -
10 UniFrac

11 **Data Availability:** All data and code used to produce the manuscript are available at
12 https://github.com/MarschmiLab/Pendleton_2025_Absolute_Unifrac_Paper, in addition to a
13 reproducible renv environment. All packages used for analysis are listed in Table S1.

14

Formatted: Font: Bold

Formatted: Line spacing: single

15 **Abstract**

16 *β -diversity is central to microbial ecology, yet commonly used metrics overlook changes in*
17 *microbial load, limiting their ability to detect ecologically meaningful shifts.* Popular for
18 incorporating phylogenetic relationships, UniFrac distances *currently* default to relative
19 abundance *and therefore omit* important variation in microbial *abundances*. As *quantifying*
20 absolute abundance *becomes more accessible, integrating* this information into β -diversity
21 analyses *is* essential. Here, we *introduce*, *Absolute UniFrac (GU^4)*, a variant of Weighted UniFrac
22 that *incorporates* absolute abundances. *Using* simulations and a *reanalysis* of four 16S rRNA
23 metabarcoding datasets (from a nuclear reactor cooling tank, the mouse gut, a freshwater lake,
24 and the peanut rhizosphere), we *demonstrate that* *Absolute UniFrac captures* microbial load,
25 composition, and phylogenetic relationships. *While this can* improve, statistical power to detect
26 ecological shifts, *we also find* *Absolute UniFrac* can be strongly correlated to differences in cell
27 abundances alone. To balance these effects, we present the generalized extension (GU^4) with a
28 tunable α parameter to *adjust the influence of abundance and composition*. Finally, we
29 benchmark GU^4 and show that although computationally slower than conventional alternatives,
30 GU^4 is comparably insensitive to realistic noise in load estimates compared to conventional
31 alternatives like Bray-Curtis dissimilarities, particularly at lower α . By coupling phylogeny,
32 composition, and microbial load, *Absolute UniFrac integrates three dimensions of ecological*
33 *change, better equipping microbial ecologists to quantitatively compare microbial communities.*

Deleted: Microbial ecologists routinely use
Deleted: metrics to compare communities, yet these metrics vary in the ecological dimensions they capture.
Deleted: , omitting
Deleted: load
Deleted: methods for
Deleted: estimating
Deleted: gain traction, incorporating
Deleted: becomes
Deleted: present
Deleted: uses
Deleted: Through
Deleted: freshwater case study.
Deleted: show that
Deleted: captures both
Deleted: s
Deleted: ,
Deleted: ing
Deleted: .
Deleted: However, it is also sensitive to variation in microbial load, especially when abundance changes occur along long branches, potentially amplifying differences. We therefore recommend a...
Deleted: form
Deleted: balance sensitivity and interpretability
Deleted: .
Deleted: ¶

61 **Main Text**

62 Microbial ecologists routinely compare communities using β -diversity metrics derived
63 from relative abundances. Yet this approach overlooks a critical ecological dimension: microbial
64 load. High-throughput sequencing produces compositional data, in which each taxon's
65 abundance is constrained by all others [1]. However, quantitative profiling studies show that cell
66 abundance, not only composition, can drive major community differences [2]. In low-biomass
67 samples, relying on relative abundance can allow contaminants to appear biologically
68 meaningful despite absolute counts too low for concern [3].

69 Sequencing-based microbiome studies therefore rely on relative abundance even when
70 the hypotheses of interest implicitly concern absolute changes in biomass. This creates a
71 mismatch between ecological framing (growth, bloom magnitude, pathogen proliferation,
72 disturbance recovery, or colonization pressure) and the information the β -diversity metric
73 encodes [4]. As a result, β -diversity is often treated as if it includes biomass, even when absolute
74 abundance is either not measured at all or is measured but excluded from the calculation (as in
75 conventional UniFrac). Many studies therefore test biomass-linked hypotheses using a metric
76 that normalizes biomass away [4]. A conceptual correction is needed in which β -diversity is
77 understood as variation along three axes: composition, phylogeny and absolute abundance.

78 Absolute microbial load measurements are now increasingly obtainable through flow
79 cytometry, qPCR, and genomic spike-ins, allowing biomass to be quantified alongside taxonomic
80 composition [4, 5]. These approaches improve detection of functionally relevant taxa and
81 mitigate the compositional constraints imposed by sequencing [1, 2]. Most studies that
82 incorporate absolute abundance counts currently rely on Bray-Curtis dissimilarity, which can
83 capture load but does not consider phylogenetic similarity [5–7]. UniFrac distances provide the
84 opposite strength, incorporating phylogeny but discarding absolute abundance, as they are
85 restricted to relative abundance data by construction [8]. This leaves no phylogenetically
86 informed β -diversity metric that operates on absolute counts, despite the fact that biomass is
87 central to many ecological hypotheses.

88 To evaluate the implications of incorporating absolute abundance into phylogenetic β -
89 diversity, we use both simulations and reanalysis of four 16S rRNA amplicon datasets. The
90 simulations use a simple four-taxon community with controlled abundance shifts to directly
91 compare both Bray-Curtis and UniFrac in their relative and absolute forms, illustrating how each
92 metric responds when abundance, composition, or evolutionary relatedness differ. We then
93 reanalyze four real-world datasets spanning nuclear reactor cooling water [5], the mouse gut [3],
94 a freshwater lake [9], and rhizosphere soil [10]. These differ widely in richness, biomass range,
95 and ecological context, allowing us to test when absolute abundance changes align with or
96 diverge from phylogenetic turnover. Together, these simulations and reanalyses provide the
97 empirical foundation for interpreting Absolute UniFrac relative to existing β -diversity measures
98 across the three axes of ecological difference: abundance, composition, and phylogeny.

99 We also extend Absolute UniFrac as was proposed by [11] to Generalized Absolute
100 UniFrac that incorporates a tunable ecological dimension, α , and evaluate its impact across
101 simulated and real-world datasets. As α increases, β -diversity is increasingly correlated with
102 differences in absolute abundance, allowing researchers to fine tune the relative weight their
103 analyses place on microbial load versus composition.

Deleted:

Deleted: {Citation}

Deleted: 1

To overcome compositional constraints, researchers increasingly use

Deleted: to quantify microbial load

Deleted: tools

Deleted: using

Deleted: dat

Deleted: a have used

Deleted: does not necessarily expect normalization to proportions

Formatted: Font: Italic

Deleted: But in the field of microbial ecology, UniFrac distances remain popular when working with relative abundance data. Here, we present *Absolute UniFrac*, a direct extension of Weighted UniFrac that incorporates total abundance, and evaluate its impact across simulated and real-world datasets.

Formatted: Indent: First line: 0.5", Line spacing: single

122 **Defining Absolute UniFrac**

123 The UniFrac distance was first introduced by Lozupone & Knight (2005) and has since
 124 become enormously popular as a measure of β -diversity within the field of microbial ecology
 125 [12]. A benefit of the UniFrac distance is that it considers phylogenetic information when
 126 estimating the distance between two communities. After first generating a phylogenetic tree
 127 representing species (or amplicon sequence variants, “ASVs”) from all samples, the UniFrac
 128 distance computes the fraction of branch-lengths which is *shared* between communities, relative
 129 to the total branch length represented in the tree. UniFrac can be both unweighted, in which only
 130 the incidence of species is considered, or weighted, wherein a branch’s contribution is weighted
 131 by the proportional abundance of taxa on that branch [8]. The Weighted UniFrac is derived:

$$U^R = \frac{\sum_{i=1}^n b_i |p_i^a - p_i^b|}{\sum_{i=1}^n b_i (p_i^a + p_i^b)}$$

132 where the contribution of each branch length, b_i , is weighted by the difference in the relative
 133 abundance of all species (p_i) descended from that branch in sample a or sample b . Here, we
 134 denote this distance as U^R , for “Relative UniFrac”. Popular packages which calculate weighted
 135 UniFrac—including the diversity-lib QIIME plug-in and the R packages phyloseq and
 136 GUniFrac—run this normalization by default [11, 13, 14].

137 Importantly, U^R is most sensitive to changes in abundant lineages, which can sometimes
 138 obscure compositional differences driven by rare to moderately-abundant taxa [11]. To address
 139 this weakness, Chen et al. (2012) introduced the generalized UniFrac distance (GU^R), in which
 140 the impact of abundant lineages can be mitigated by decreasing the parameter α :

$$GU^R = \frac{\sum_{i=1}^n b_i (p_i^a + p_i^b)^\alpha |p_i^a - p_i^b|}{\sum_{i=1}^n b_i (p_i^a + p_i^b)^\alpha}$$

141 where α ranges from 0 (close to Unweighted UniFrac) up to 1 (identical to U^R , above). However,
 142 if one wishes to use absolute abundances, both U^R and GU^R can be derived without normalizing
 143 to proportions:

$$U^A = \frac{\sum_{i=1}^n b_i |c_i^a - c_i^b|}{\sum_{i=1}^n b_i (c_i^a + c_i^b)} \quad GU^A = \frac{\sum_{i=1}^n b_i (c_i^a + c_i^b)^\alpha |c_i^a - c_i^b|}{\sum_{i=1}^n b_i (c_i^a + c_i^b)^\alpha}$$

144 Where c_i^a and c_i^b denote for the absolute counts of species descending from branch b_i in
 145 communities a and b , respectively. We refer to these distances as *Absolute UniFrac* (U^A) and
 146 *Generalized Absolute UniFrac* (GU^A). Although substituting absolute for relative abundances is
 147 mathematically straightforward, we found no prior work that examines UniFrac in the context of
 148 absolute abundance, either conceptually or in application. Incorporating absolute abundances
 149 introduces a third axis of ecological variation: beyond differences in composition and
 150 phylogenetic similarity, U^A also captures divergence in microbial load. This makes interpretation
 151 of U^A nontrivial, particularly in complex microbiomes.

152 **Demonstrating β -diversity metrics’ behavior with a simple simulation**

153 Formatted: Line spacing: single

Deleted:

154 Formatted: Indent: First line: 0.5", Line spacing: single

Deleted: s

155 Formatted: Line spacing: single

Deleted: we weight the length

Deleted: f

Deleted: Because

Deleted: it

156 Formatted: Indent: First line: 0.5", Line spacing: single

157 Formatted: Line spacing: single

Deleted: stands

Deleted: ed

Deleted: y

Deleted: f

Deleted:

Deleted: U^A and

158 Formatted: Font: Bold

168 To clarify how U^A behaves relative to existing β -diversity metrics, we first constructed a
169 simple four-taxon simulated community arranged in a small phylogeny (Fig. 1A). By varying the
170 absolute abundance of each ASV (1, 10, or 100), we generated 81 samples and 3,240 pairwise
171 comparisons. For each pair, we computed four dissimilarity metrics: Bray-Curtis with relative
172 abundance (BC^R), Bray-Curtis with absolute abundance (BC^A), Weighted UniFrac with relative
173 abundance (U^R), and Weighted UniFrac with absolute abundance (U^A). These comparisons help
174 to illustrate how each axis of ecological difference—abundance, composition, and phylogeny—is
175 expressed by the different metrics.

176 U^A does not consistently yield higher or lower distances compared to other metrics, but
177 instead varies depending on how abundance and phylogeny intersect (Fig. 1B). In the improbable
178 scenario that all branch lengths are equal, U^A is always less than or equal to BC^A (Fig. S1).
179 These comparisons emphasize that once branch lengths differ, incorporating phylogeny and
180 absolute abundance alters the structure of the distance space. The direction and magnitude of that
181 change depend on which branches carry the abundance shifts. U^A is also usually smaller than
182 BC^A and is more strongly correlated with BC^A (Pearson's $r = 0.82$, $p < 0.0001$) than with BC^R (r
183 = 0.41) and U^R ($r = 0.55$).

184 To better understand how these metrics diverge, we examined individual sample pairs
185 (Fig. 1C). Scenario 1 (gold star) illustrates the classic advantage of UniFrac: ASV_1 and ASV_2
186 are phylogenetically close, so U^R and U^A discern greater similarity between samples than BC^R
187 and BC^A , which ignore phylogenetic structure. Scenario 2 (red star) highlights a limitation of
188 relative metrics: two samples with identical relative composition but a 100-fold difference in
189 biomass appear identical to BC^R and U^R , but not to their absolute counterparts. In Scenario 3
190 (green star), incorporating absolute abundance decreases dissimilarity. BC^A and U^A are lower
191 than their relative counterparts because half the community is identical in absolute abundance,
192 even though their proportions differ. In contrast, Scenario 4 (blue star) shows that U^A can exceed
193 BC^A when abundance differences occur on long branches, amplifying phylogenetic dissimilarity.

194 These scenarios demonstrate that U^A integrates variation along three ecologically
195 relevant axes: composition, phylogenetic similarity, and microbial load, rather than isolating any
196 single dimension. Because a given U^A value can reflect multiple drivers of community change,
197 interpreting it requires downstream analyses to disentangle the relative contributions of these
198 three axes. To evaluate how this plays out in real systems we next reanalyzed four previously
199 published datasets spanning diverse microbial environments.

Formatted: Indent: First line: 0.5", Line spacing: single

Deleted: To illustrate how U^A behaves, we constructed a simulated community of four ASVs arranged in a simple phylogeny (Fig. 1A).

Deleted:

Deleted: reshapes distance estimates in nontrivial ways.

Deleted:

Deleted: terms, despite proportional differences

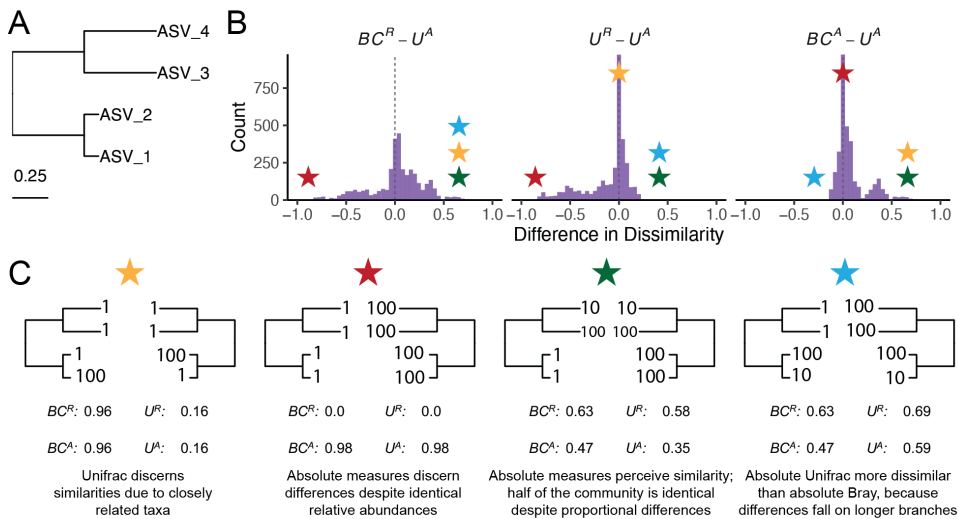
Deleted: increase dissimilarity relative to

Deleted: ¶

Formatted: Indent: First line: 0"

Formatted: Indent: First line: 0.5", Line spacing: single

Deleted: ¶



213 *Figure 1. Simulated communities reveal how absolute abundance affects phylogenetic and non-phylogenetic β -*
214 *diversity measures.* (A) We constructed a simple four-ASV community with a known phylogeny and generated all
215 permutations of each ASV having an absolute abundance of 1, 10, or 100, resulting in 81 unique communities and
216 3,240 pairwise comparisons. (B) Distributions of pairwise differences between weighted UniFrac using absolute
217 abundance (U^A) and three other metrics: Bray-Curtis using relative abundance (BC^R), weighted UniFrac using
218 relative abundance (U^R), and Bray-Curtis using absolute abundance (BC^A). (C) Illustrative sample pairs demonstrate
219 how absolute abundances and phylogenetic structure interact to increase or decrease dissimilarity across metrics.
220 Stars indicate where each scenario falls within the distributions shown in panel B. Actual values for each metric are
221 displayed beneath each scenario.

Application of Absolute UniFrac to Four Real-World Microbiome Datasets

223 To illustrate the sensitivity of U^A to both variation in composition and absolute
224 abundance, we re-analyzed four previously published datasets from diverse microbial systems.
225 These datasets included: (i) nuclear reactor cooling water sampled across three reactor cycle
226 phases [5]; (ii) the mouse gut sampled across multiple regions and between two diets [3]; (iii)
227 depth-stratified freshwater communities sampled across two months [9]; and (iv) peanut
228 rhizospheres under two crop rotation schemes (conventional rotation (CR) vs. sod-based rotation
229 (SBR)), plant maturities, and irrigation treatments [10]. Absolute abundance was quantified by
230 flow cytometry for the cooling water and freshwater datasets, droplet digital PCR for the mouse
231 gut, and by qPCR for the rhizosphere dataset. Together these span a wide range of richness—from
232 215 ASVs in the cooling water to 24,000 ASVs in the soil—and microbial load—from as low as
233 4×10^5 cells/ml (cooling water) up to 2×10^{12} 16S rRNA copies/gram (mouse gut). Additional

Formatted: Line spacing: single

Deleted: Example comparisons i

Deleted: ng specific scenarios where U^A yields greater or smaller dissimilarity than other metrics.

Deleted: Colored s

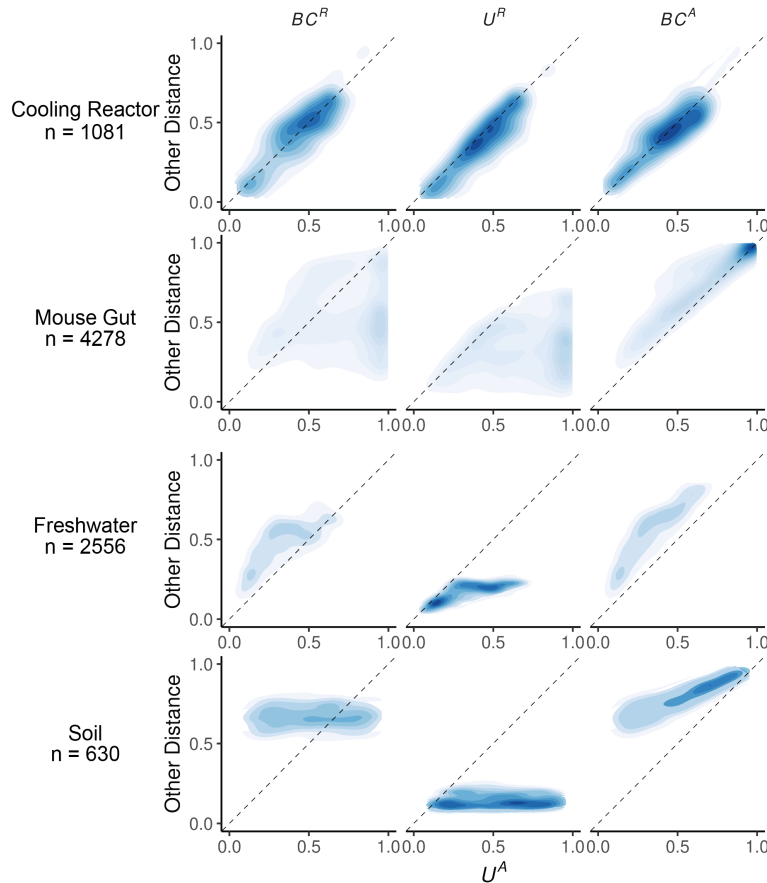
Deleted: Across all 3,240 pairwise comparisons, U^A is usually smaller than and strongly correlated with BC^A (Pearson's $r = 0.82$, $p < 0.0001$) than with BC^R ($r = 0.41$) and U^R ($r = 0.55$), reflecting the effect illustrated in Scenario 1. However, exceptions like Scenario 4 show that U^A can also yield larger distances than BC^A when abundance differences occur on long branches. These scenarios demonstrate that U^A

Formatted: Font: Bold

Formatted: Indent: First line: 0", Line spacing: single

246 details of the re-analysis workflow, including ASV generation and phylogenetic inference, are
247 provided in the Supporting Methods.

Formatted: Font: 10 pt



248
249
250
251
252
253
254 *Figure 2. Absolute UniFrac (U^A) compared with other β -diversity metrics across four real microbial datasets. Each*
panel shows pairwise sample distances for U^A (x-axis) against another metric (y-axis): Bray-Curtis using relative
abundance (BC^R , first column), weighted UniFrac using relative abundances (U^R , second column), and Bray-Curtis
using absolute abundances (BC^A , third column). Contours indicate the relative density of pairwise comparisons (n
shown for each dataset, left), with darker shading corresponding to more observations. The dashed line marks the
1:1 relationship. Points above the line indicate cases where U^A is smaller than the comparator metric, while points
below the line indicate cases where U^A is larger.

Formatted: Indent: First line: 0", Line spacing: single

255 We first calculated four β -diversity metrics for all sample pairs in each dataset and
256 compared them to U^A (Fig. 2). The degree of concordance between U^A and other metrics was
257 highly context dependent. In the cooling water dataset, U^A closely tracked all three alternatives,
258 whereas in the remaining systems it diverged substantially. U^A also spanned a similar or wider

Formatted: Font: 10 pt

Formatted: Line spacing: single

range of distances than the other metrics. For example, in the soil dataset BC^R and U^R occupied a narrow range relative to the broad separation observed under U^A .

U^A generally reported distances that were similar to or greater than U^R , consistent with the simulations shown in Fig. 1B. This reflects the ability of U^A to discern dissimilarity due to differences in microbial load, even when community composition is conserved. In contrast, U^A yielded distances that were similar to or lower than BC^A , again matching the simulated behavior in Fig 1B. In these cases, phylogenetic proximity between abundant, closely-related ASVs leads U^A to register greater similarity than BC^A .

Given these differences, we next quantified how well each metric discriminates among categorical sample groups. For each dataset, we ran PERMANOVAs to measure the proportion of variance (R^2) and statistical power (*pseudo-F*, *p*-value) attributable to group structure, using groupings that were determined to be significant in the original publications. To evaluate how strongly absolute abundance contributed to this discrimination, we also calculated GU^A across a range of α values. The resulting R^2 values are displayed in Fig. 3A, with the corresponding *pseudo-F* statistics and *p*-values provided in Fig. S2.

As in Fig. 2, the performance of each metric was strongly context dependent (Fig. 3A). In the mouse gut and freshwater datasets, absolute-abundance-aware metrics (BC^A and GU^A) explained the greatest proportion of variance (R^2), and R^2 generally increasing as α increased. In contrast, relative metrics captured more variation in the cooling water dataset (again at higher α), and all metrics explained comparably little variance in the soil dataset. Taken at face value, these trends might suggest that higher α values typically improve group differentiation.

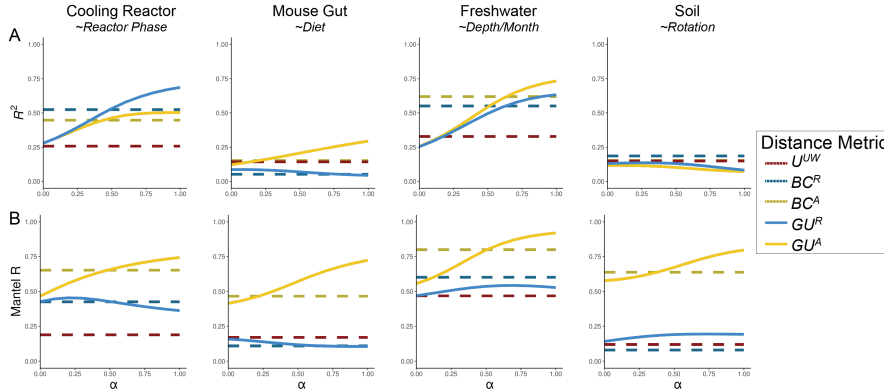
However, this comes with a major caveat: at high α values, GU^A becomes strongly correlated with total cell count alone (Fig. 3B). Mantel tests confirmed that absolute-abundance metrics are far more sensitive to differences in microbial load than their relative counterparts. This behavior is intuitive, and to some extent desirable, because these metrics are designed to detect changes in microbial load even when composition remains constant. Yet at $\alpha = 1$, U^A approaches a proxy for sample absolute abundance itself. In ordination space (Fig. S3), this can cause Axis 1 to correlate with absolute abundance and in some cases (freshwater and soil) produces strong horseshoe effects [15], potentially distorting ecological interpretation.

Deleted: integrates ecological realism by capturing differences in both lineage identity and total biomass.[¶]

Moved (insertion) [1]

Deleted: We next evaluated how U^A influences group separation in a real-world dataset. Using a previously published 16S rRNA gene dataset from Lake Ontario, we analyzed 66 samples and >7,000 ASVs. Samples clustered into three groups defined by depth and month, reflecting shifts in both taxonomic composition and microbial load (Fig. S2, [10]). Our goal was to determine whether weighting phylogenetic distances by absolute abundance enhances interpretability and statistical power to distinguish sample groups.[¶] with total cell count alone (Fig. 2D). Mantel tests showed that absolute distance metrics are much more sensitive to differences in cell counts than their relative counterparts. This is intuitive, and to a degree, intentional: these metrics aim to detect changes in biomass even when composition remains constant. Yet at $\alpha = 1$, U^A is nearly a proxy for sample biomass. In ordination space, this manifests as Axis 1 being almost perfectly correlated with absolute abundance (Spearman's $\rho = -1.0$), whereas at $\alpha = 0.0$, the correlation is moderate ($\rho = 0.58$). The structure observed in Fig. 2A at $\alpha = 1$ may largely reflect a horseshoe effect [14], where a strong gradient (here, cell counts) becomes curved in ordination space, potentially distorting ecological interpretation.[¶]

UniFrac (GU^A) across three levels of α : 0.0 (approximating unweighted UniFrac), 0.5, and 1.0 (equivalent to U^A). As α increased, PCoA ordinations revealed stronger similarity between Shallow May and Shallow September samples, reflecting their higher cell counts compared to the Deep samples (Fig. 2A). Notably, the proportion of variation explained by the first PCoA axis increased substantially with α , going from 18.3% at $\alpha = 0$ up to 76.7% $\alpha = 1$. This trend was also true for U^R across multiple α , but to a much weaker degree (Fig. S3).



325 *Figure 3. Discriminatory performance of U^A and related metrics across four microbial systems.* (A) PERMANOVAs
 326 were used to quantify the percent variance (R^2) explained by predefined categorical groups (shown in italics beneath
 327 each dataset name), with 1,000 permutations. Metrics were evaluated across five metrics and, where applicable,
 328 across eleven α values (0–1 in 0.1 increments). For consistency with the original studies, only samples from Reactor
 329 cycle 1 were used for the cooling-water dataset, only stool samples for the mouse gut dataset, and only mature
 330 rhizosphere samples for the dataset. (B) Mantel correlation (R) between each distance metric and the pairwise
 331 differences in absolute abundance (cell counts or 16S copy number), illustrating the degree to which each metric is
 332 driven by biomass differences.

333 We recommend calibrating α based on research goals, modulating this effect by using
 334 GU^A across a range of α rather than relying on U^A ($\alpha = 1$). Researchers should consider how
 335 much emphasis they want their dissimilarity metric to place on microbial load (Box 1). When
 336 biomass differences are central to the hypothesis being tested (for example, detecting
 337 cyanobacterial blooms), high α are recommended. In contrast, if microbial load is irrelevant or
 338 independent of the hypothesis in question, low α (or U^R) may be preferred; for example in the
 339 soil dataset, fine-scale differences in composition may be obscured by random variation in
 340 microbial load.

341 In many systems, microbial biomass is one piece of the story, likely correlated to other
 342 variables being tested. If the importance of microbial load in the system is unknown, one
 343 potential approach is to calculate correlations as demonstrated in Fig. 3B and select an α prior to
 344 any ordinations or statistical testing. Again, absolute metrics are expected to correlate to
 345 differences in cell count, as we hope absolute abundance measures incorporate differences in cell
 346 counts, especially when microbial load is relevant to the hypotheses being tested. Correlations to
 347 cell count in BC^A , an accepted approach in the literature, ranged from ~0.5 up to ~0.8. As a
 348 general recommendation from these analyses, we recommend α values in an intermediate range
 349 from 0.1 up to 0.6.

350 Computational and Methodological Considerations

351 Applying GU^A in practice raises several considerations related to sequencing depth,
 352 richness, and computational cost. Both Bray-Curtis and UniFrac can be sensitive to sequencing
 353 depth because richness varies with read count [16–18]. Methods to address these concerns,
 354 including rarefaction, remain debated and are challenging to benchmark rigorously [19]. We do
 355 not evaluate the sensitivity of U^A or GU^A to different rarefaction strategies here, but we do

Formatted: Font: 10 pt

Formatted: Indent: First line: 0", Line spacing: single

Moved up [1]: at high α values, GU^A became strongly correlated with total cell count alone (Fig. 2D). Mantel tests showed that absolute distance metrics are much more sensitive to differences in cell counts than their relative counterparts. This is intuitive, and to a degree, intentional: these metrics aim to detect changes in biomass even when composition remains constant. Yet at $\alpha = 1$, U^A is nearly a proxy for sample biomass. In ordination space, this manifests as Axis 1 being almost perfectly correlated with absolute abundance (Spearman's $\rho = -1.0$), whereas at $\alpha = 0.0$, the correlation is moderate ($\rho = 0.58$). The structure observed in Fig. 2A at $\alpha = 1$ may largely reflect a horseshoe effect [12], where a strong gradient (here, cell counts) becomes curved in ordination space, potentially distorting ecological interpretation.

Deleted:

To quantify the impact on group differentiation, we performed PERMANOVA across depth-month groupings using GU^R , GU^A , BC^R , and BC^A at varying α (Fig. 2B–C). Across all metrics, incorporating absolute abundance increased both the proportion of explained variance (R^2) and the pseudo F -statistic. GU^A achieved a maximum R^2 of 75.8% and a pseudo F -statistic 1.56 times greater than GU^R , highlighting the ability of GU^A to detect group differences driven by microbial load.¹

However, a major caveat emerged:

Deleted:

Deleted: urge careful calibration of

Deleted: thereby mitigating

Formatted: Line spacing: single

Deleted:

Formatted: Indent: First line: 0.5", Line spacing: single

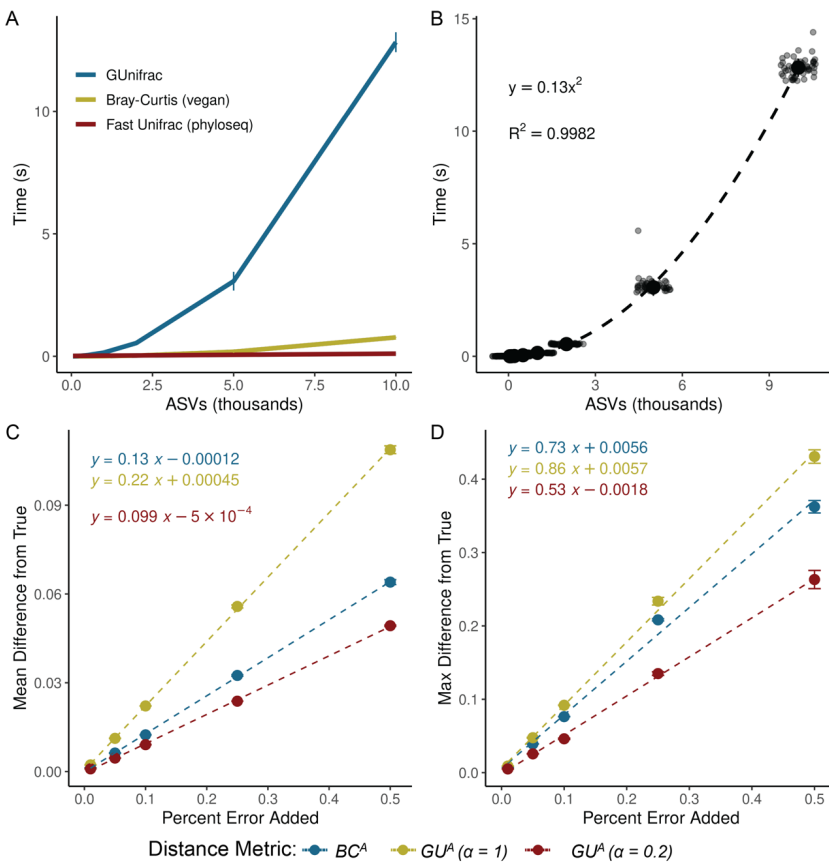
Deleted: In this dataset, we recommend an intermediate α of 0.5, consistent with prior guidance [9], but especially important when using absolute abundance data.

Deleted:

Formatted: Font: Bold

Formatted: Line spacing: single

429 provide a workflow and code for how we incorporated rarefaction into our own analyses (Box 2
 430 and available code). This approach minimizes sequencing-depth biases while preserving
 431 abundance scaling for downstream β -diversity analysis.



432

433 *Figure 4. GU^A requires more computational time but remains resilient to quantification error. (A) Runtime for GU^A*
 434 (*GUUnifrac package*), U^R (*FastUniFrac* in the *phyloseq* package) and BC^A (*vegan* package) was benchmarked across
 435 50 iterations on a sub-sampled soil dataset (mature samples only) [10], using increasing ASV richness (50, 100, 200,
 436 500, 1,000, 2,000, 5,000, 10,000), with 10 samples and one α value per run (unweighted UniFrac is also calculated
 437 by default). Error bars represent standard deviation. (B) Quadratic relationship between GU^A computation time and
 438 ASV richness. Large center point represents median across 50 iterations, error bars (standard deviation) are too
 439 small to be seen. (C-D) Sensitivity of GU^A ($\alpha = 1$ and 0.2) and BC^A to measurement error was evaluated by adding
 440 random variation ($\pm 1\%$ to $\pm 50\%$; Supporting Methods) to 16S copy number estimates in stool samples from the
 441 mouse gut dataset [3]. For each error level, 50 replicate matrices were generated and compared to the original
 442 values. Panels reflect the (C) mean difference and (D) max difference between the error-added metrics compared to
 443 the originals. Error bars represent the standard deviation of the average mean and max difference across 50
 444 iterations.

445 *GU^A* is slower to compute than both BC^A and U^R because it must traverse the phylogenetic
446 tree to calculate branch lengths for each iteration. Computational time of GU^A increases
447 quadratically with ASV number and is 10-20 times slower, though up to 50 times slower, than
448 BC^A (Fig. 4A-B). The number of samples or α values, however, have relatively little effect on
449 runtime (Fig. S4). For a dataset of 24,000 ASVs, computing on a single CPU is still reasonable
450 (1.4 minutes), but repeated rarefaction increases runtime substantially because branch lengths are
451 redundantly calculated with each iteration. Allowing branch-length objects to be cached or
452 incorporated directly into the GUnifrac workflow would considerably improve computational
453 efficiency.

454 We also evaluated the sensitivity of GU^A to measurement error in absolute abundance due to
455 uncertainty arising from the quantification of cell number of 16S copy number. To assess the
456 sensitivity of GU^A and BC^A to measurement error, we added random error to the 16S copy
457 number measurements from the mouse gut dataset, limiting our analyses to the stool samples
458 where copy numbers varied by an order of magnitude. Across 50 iterations, each copy number
459 could randomly vary by a given percentage of error in either direction. We re-calculated β -
460 diversity (BC^A and GU^A at $\alpha = 1$ and $\alpha = 0.2$) and compared these measurements to the original
461 dataset.

462 Introducing random variation into measured 16S copy number altered GU^A values only
463 modestly, and the effect was proportional to the magnitude of the added noise (Fig. 4C-D). At α
464 = 1, each 1% of quantification error introduced an average difference of 0.0022 in GU^A ; at $\alpha =$
465 0.2, GU^A was even less sensitive. Thus, moderate α values provide a balance between
466 interpretability and robustness to noise in absolute quantification. The max deviation from true
467 that added error could inflict on a given metric was also proportional (and always less) than the
468 magnitude of the error itself (Fig. 4D). A more rigorous approach to assessing error propagation
469 within these metrics, including mathematical proofs of the relationships estimated above, is
470 outside the scope of this paper but would be helpful.

471 Ecological Interpretation and conceptual significance

472 Absolute UniFrac reframes the interpretation of β -diversity by making biomass an explicit
473 ecological axis rather than an unmeasured or normalized-away quantity. Conventional UniFrac
474 capture composition and shared evolutionary history, but implicitly invites interpretation as if it
475 also encodes differences on microbial load. By incorporating absolute abundance directly,
476 Absolute UniFrac helps to resolve this mismatch and restores alignment between ecological
477 hypotheses and the quantities represented in the metric. In this view, β -diversity becomes a three-
478 axis ecological measure, incorporating composition, phylogeny and biomass, rather than a two-
479 axis approximation. That said, the additional dimension of microbial load also increases the
480 complexity of applying and interpreting this metric.

481 There are many cases where the incorporation of absolute abundance allows microbial
482 ecologists to assess more realistic, ecologically-relevant differences in microbial communities,
483 especially when microbial load is mechanistically central. Outside of the datasets re-analyzed
484 here [3, 5, 9, 10], the temporal development of the infant gut microbiome involves both a rise in
485 absolute abundance and compositional changes [6]; bacteriophage predation in wastewater
486 bioreactors can be understood only when microbial load is considered [20]; and antibiotic-driven
487 declines in specific swine gut taxa were missed using relative abundance approaches [21]. As β -

Formatted: Indent: First line: 0.5", Space After: 8 pt,
Adjust space between Latin and Asian text, Adjust space
between Asian text and numbers, Tab stops: Not at 0.39" +
0.78" + 1.17" + 1.56" + 1.94" + 2.33" + 2.72" + 3.11" +
3.5" + 3.89" + 4.28" + 4.67"

Formatted: Font: Not Italic

Formatted: Font: Not Italic

Formatted: Font: (Default) Times New Roman

Formatted: Font: (Default) Times New Roman

Formatted: Font: (Default) Times New Roman

Formatted: Line spacing: single

Formatted: Indent: First line: 0.35", Line spacing: single

Formatted: Font: 10 pt

Deleted: [11][3]

489 diversity metrics (and UniFrac specifically) remain central to microbial ecology, these findings
490 highlight how interpretation changes once biomass is incorporated. Broader adoption of absolute
491 abundance profiling will also depend on data availability. Few studies currently make absolute
492 quantification data publicly accessible, underscoring the need to deposit absolute measurements
493 alongside sequencing reads for reproducibility, ideally as metadata within SRA submissions.

494 While demonstrated here with 16S rRNA data, the approach should extend to other marker
495 genes or (meta)genomic features, provided absolute abundance estimates are available. In this
496 sense, GU^A offers a more ecologically grounded view of lineage turnover by jointly reflecting
497 variation in biomass and phylogenetic structure.

498 No single metric (or α in GU^A), however, is universally “best”. Each β -diversity metric
499 emphasizes a different dimension of community change. Researchers should therefore select
500 metrics based on the ecological quantity that is hypothesized to matter most. Here, we
501 demonstrate not that GU^A outperforms other measures, but that it faithfully incorporates the three
502 axes of variation it was designed to incorporate: composition, phylogenetic similarity, and
503 absolute abundance (Fig. 1 and Fig. 2). As with any β -diversity analysis, interpretation requires
504 matching the metric to the ecological question at hand, and exploring sensitivity across different
505 metrics where appropriate [22]. By providing demonstrations and code for the application and
506 interpretation of U^A/GU^A , we hope to encourage the use of these metrics as a tool of microbial
507 ecology.

508 Conclusion

509 By explicitly incorporating absolute abundance, Absolute UniFrac shifts phylogenetic β -
510 diversity from a two-axis approximation to a three-axis ecological measure. This reframing
511 connects the metric to the underlying biological questions that motivate many microbiome
512 studies. As methods for quantifying microbial load continue to expand, the ability to interpret β -
513 diversity in a biomass-aware framework will become increasingly important for distinguishing
514 true ecological turnover from proportional change alone. In this way, Absolute UniFrac is not
515 simply an alternative distance metric but a tool for aligning statistical representation with
516 ecological mechanism.

517

Formatted: Indent: First line: 0.35", Line spacing: single

Deleted:

Formatted: Line spacing: single

Formatted: Font: Not Italic

520 **Box 1: β -diversity metrics should reflect the hypothesis being tested**

Formatted: Font: Bold

521 Absolute UniFrac is most informative when variation in microbial load is expected to carry
 522 ecological meaning rather than being a nuisance variable. The choice of α determines how
 523 strongly abundance differences influence the metric, and should therefore be selected based on
 524 the hypothesis, not by convention. In settings where biomass is central to the mechanism under
 525 study, higher α values appropriately foreground that signal, whereas in cases where load
 526 variation is incidental or confounding, lower α values maintain interpretability. Framing α as a
 527 hypothesis-driven choice repositions β -diversity from a default normalization step to an explicit
 528 ecological decision.

			Metric to Use			Hypothetical Example
			<u>Central to hypothesis</u>			<u>$GU^A, \alpha > 0.5$</u>
			<u>Relevant, but associated with other variables of interest</u>			<u>$GU^A, 0.1 < \alpha < 0.5$</u>
Treat closely related lineages as similar?	Yes	How relevant is microbial load?	Irrelevant	Emphasize rare or dominant taxa?	Dominant	<u>$GU^R, \alpha > 0.5$</u>
				Rare		<u>$GU^R, \alpha < 0.5$</u>
			<u>Unknown</u>			<u>GU^A at multiple α</u>
	No	Microbial load relevant?	Yes			<u>Random variation in microbial load obscures compositional shifts in soil communities</u>
			No			<u>Strain turnover and proliferation in the infant gut</u>
						<u>Temporal succession in chemostat</u>

Formatted: Font: 10 pt

Formatted: Font: 10 pt

Formatted: Centered

Formatted: Font: 10 pt

Formatted: Font: 10 pt

Formatted: Centered

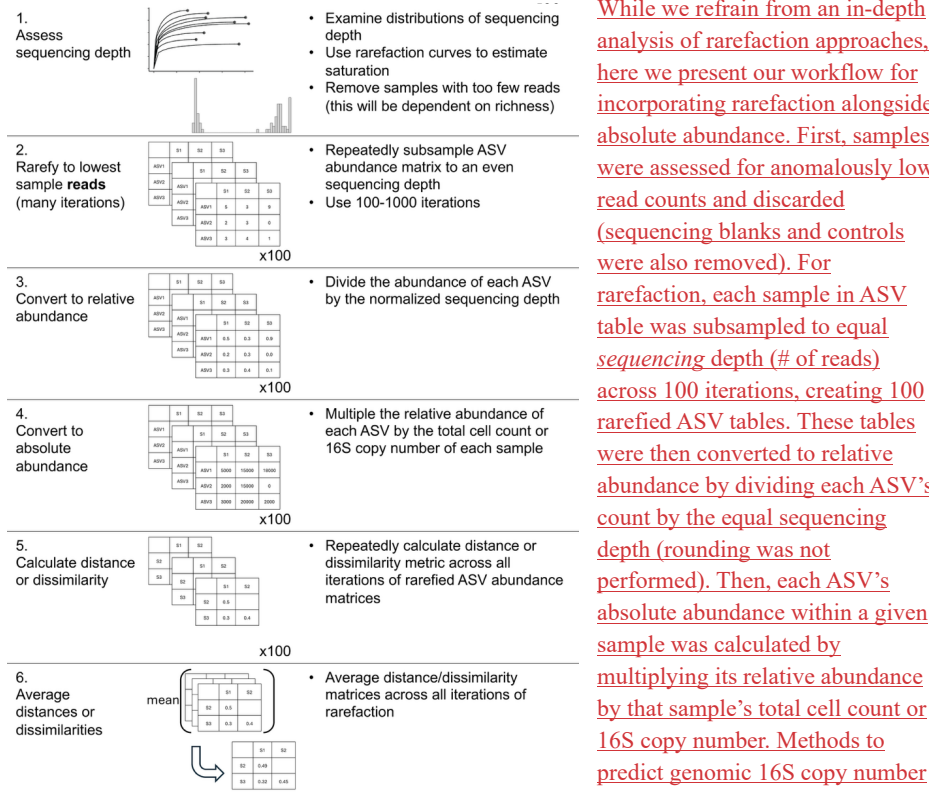
Formatted: Font: 10 pt, Not Italic

Formatted: Font: 10 pt

Formatted: Centered

532 Box 2: Rarefaction workflow for incorporating absolute abundance

Formatted: Font: Bold



While we refrain from an in-depth analysis of rarefaction approaches, here we present our workflow for incorporating rarefaction alongside absolute abundance. First, samples were assessed for anomalously low read counts and discarded (sequencing blanks and controls were also removed). For rarefaction, each sample in ASV table was subsampled to equal sequencing depth (# of reads) across 100 iterations, creating 100 rarefied ASV tables. These tables were then converted to relative abundance by dividing each ASV's count by the equal sequencing depth (rounding was not performed). Then, each ASV's absolute abundance within a given sample was calculated by multiplying its relative abundance by that sample's total cell count or 16S copy number. Methods to predict genomic 16S copy number for a given ASV were not used

559 [23]. Each distance/dissimilarity metric was then calculated across all 100 absolute-normalized
 560 ASV tables. The final distance/dissimilarity matrix was calculated by averaging all 100 iterations
 561 of each distance/dissimilarity calculation. Of note for future users: pruning the phylogenetic tree
 562 after rarefaction for each iteration is not necessary – ASVs removed from the dataset do not
 563 contribute nor change the calculated of UniFrac distances.

565

566

567 **References**

- 568 1. Gloor GB et al. Microbiome Datasets Are Compositional: And This Is Not Optional. *Front
569 Microbiol* 2017;8:2224. <https://doi.org/10.3389/fmicb.2017.02224>
- 570 2. Vandepitte D et al. Stool consistency is strongly associated with gut microbiota richness
571 and composition, enterotypes and bacterial growth rates. *Gut* 2016;65:57–62.
<https://doi.org/10.1136/gutjnl-2015-309618>
- 572 3. Barlow JT, Bogatyrev SR, Ismagilov RF. A quantitative sequencing framework for absolute
573 abundance measurements of mucosal and luminal microbial communities. *Nat Commun*
574 2020;11:2590. <https://doi.org/10.1038/s41467-020-16224-6>
- 575 4. Wang X et al. Current Applications of Absolute Bacterial Quantification in Microbiome
576 Studies and Decision-Making Regarding Different Biological Questions. *Microorganisms*
577 2021;9:1797. <https://doi.org/10.3390/microorganisms9091797>
- 578 5. Props R et al. Absolute quantification of microbial taxon abundances. *ISME J* 2017;11:584–
579 587. <https://doi.org/10.1038/ismej.2016.117>
- 580 6. Rao C et al. Multi-kingdom ecological drivers of microbiota assembly in preterm infants.
581 *Nature* 2021;591:633–638. <https://doi.org/10.1038/s41586-021-03241-8>
- 582 7. Bray JR, Curtis JT. An Ordination of the Upland Forest Communities of Southern
583 Wisconsin. *Ecological Monographs* 1957;27:326–349. <https://doi.org/10.2307/1942268>
- 584 8. Lozupone CA et al. Quantitative and Qualitative β Diversity Measures Lead to Different
585 Insights into Factors That Structure Microbial Communities. *Applied and Environmental
586 Microbiology* 2007;73:1576–1585. <https://doi.org/10.1128/AEM.01996-06>

Formatted: Line spacing: single

Deleted: That said, interpretation of GU^A requires care. When biomass differences dominate, ordinations may largely reflect microbial load rather than lineage turnover, particularly at $\alpha = 1$ and with long phylogenetic branches. In such cases, higher statistical power may come at the cost of biological nuance. We also do not address related concerns, such as how sequencing depth influences richness estimates or whether rarefaction should be applied before calculating GU^A [15]. As with any β -diversity study, researchers should interpret results critically, explore sensitivity across metrics, and justify their choice of α [16]. Our results suggest that an intermediate α value offers a practical compromise that balances sensitivity to biomass with robustness to overdominance by total load, especially when lineage turnover is also of interest. We anticipate that GU^A will become an essential tool for microbiome researchers seeking to incorporate absolute abundance into ecologically grounded β -diversity comparisons.¶

- 606 9. Pendleton A, Wells M, Schmidt ML. Upwelling periodically disturbs the ecological
607 assembly of microbial communities in the Laurentian Great Lakes. 2025. bioRxiv, 2025. ,
608 2025.01.17.633667
- 609 10. Zhang K et al. Absolute microbiome profiling highlights the links among microbial
610 stability, soil health, and crop productivity under long-term sod-based rotation. *Biol Fertil
611 Soils* 2022;58:883–901. <https://doi.org/10.1007/s00374-022-01675-4>
- 612 11. Chen J et al. Associating microbiome composition with environmental covariates using
613 generalized UniFrac distances. *Bioinformatics* 2012;28:2106–2113.
614 <https://doi.org/10.1093/bioinformatics/bts342>
- 615 12. Lozupone C, Knight R. UniFrac: a New Phylogenetic Method for Comparing Microbial
616 Communities. *Applied and Environmental Microbiology* 2005;71:8228–8235.
617 <https://doi.org/10.1128/AEM.71.12.8228-8235.2005>
- 618 13. McMurdie PJ, Holmes S. phyloseq: An R package for reproducible interactive analysis and
619 graphics of microbiome census data. *PLoS ONE* 2013;8:e61217.
- 620 14. Bolyen E et al. Reproducible, interactive, scalable and extensible microbiome data science
621 using QIIME 2. *Nat Biotechnol* 2019;37:852–857. [https://doi.org/10.1038/s41587-019-0209-9](https://doi.org/10.1038/s41587-019-
622 0209-9)
- 623 15. Morton JT et al. Uncovering the Horseshoe Effect in Microbial Analyses. *mSystems*
624 2017;2:10.1128/msystems.00166-16. <https://doi.org/10.1128/msystems.00166-16>
- 625 16. Schloss PD. Evaluating different approaches that test whether microbial communities have
626 the same structure. *The ISME Journal* 2008;2:265–275.
627 <https://doi.org/10.1038/ismej.2008.5>

- 628 17. Fukuyama J et al. Comparisons of distance methods for combining covariates and
629 abundances in microbiome studies. *Biocomputing 2012*. WORLD SCIENTIFIC, 2011,
630 213–224.
- 631 18. McMurdie PJ, Holmes S. Waste Not, Want Not: Why Rarefying Microbiome Data Is
632 Inadmissible. *PLOS Computational Biology* 2014;10:e1003531.
633 <https://doi.org/10.1371/journal.pcbi.1003531>
- 634 19. Schloss PD. Waste not, want not: revisiting the analysis that called into question the
635 practice of rarefaction. *mSphere* 2023;9:e00355-23. <https://doi.org/10.1128/mSphere.00355-23>
- 637 20. Shapiro OH, Kushmaro A, Brenner A. Bacteriophage predation regulates microbial
638 abundance and diversity in a full-scale bioreactor treating industrial wastewater. *The ISME
639 Journal* 2010;4:327–336. <https://doi.org/10.1038/ismej.2009.118>
- 640 21. Wagner S et al. Absolute abundance calculation enhances the significance of microbiome
641 data in antibiotic treatment studies. *Front Microbiol* 2025;16.
642 <https://doi.org/10.3389/fmicb.2025.1481197>
- 643 22. Kers JG, Saccenti E. The Power of Microbiome Studies: Some Considerations on Which
644 Alpha and Beta Metrics to Use and How to Report Results. *Front Microbiol* 2022;12.
645 <https://doi.org/10.3389/fmicb.2021.796025>
- 646 23. Douglas GM et al. PICRUSt2 for prediction of metagenome functions. *Nat Biotechnol*
647 2020;38:685–688. <https://doi.org/10.1038/s41587-020-0548-6>
- 648

Page 9: [1] Deleted

Augustus Raymond Pendleton

9/28/25 9:44:00 PM